Journal of Applied Polymer Science

Synthesis of metal-free poly(*p*-dioxanone) by phosphazene base catalyzed ring-opening polymerization

Hongjun Yang, Tao Bai, Xiaoqiang Xue, Wenyan Huang, Jianhai Chen, Bibiao Jiang
School of Materials Science and Engineering, Jiangsu Key Laboratory of Materials Surface Science and Technology, Jiangsu Collaborative Innovation Center of Photovolatic Science and Engineering, Changzhou University, Changzhou, Jiangsu, 213164, P. R. China
Correspondence to: B. Jiang (E-mail: jiangbibiao@cczu.edu.cn)

ABSTRACT: Poly(*p*-dioxanone) (PPDO) has received significant attention due to its good biocompatibility and fast biodegradation profiles. In addition, PPDO is a polymer with high potential in biomedical applications. However, the conventional syntheses of PPDO via the ring-opening polymerization (ROP) of *p*-dioxanone (PDO) often use a metallic catalyst, which significantly limits its biorelated applications. This investigation was focused on the synthesis of metal-free PPDO by using phosphazene base *t*-BuP_4 as the catalyst. The effects of the reaction conditions including temperature, reaction time, initiators, and feed molar ratios were studied in detail by nuclear magnetic resonance spectroscopy, viscosimetry, differential scanning calorimetry, and thermogravimetric analysis. The results showed that *t*-BuP_4 exhibited especially high activity in catalyzing alcohol or aniline to initiate the ROP of PDO, consequently resulting in metal-free PPDOs. The polymerization was optimum at a reaction temperature of approximately 100°C and 88.7% of PDO was consumed. The viscosity–average molecular weights of the resulting polymer reached as high as 2.09×10^4 g/mol. The molar ratios of [PDO]/[*t*-BuP_4] also had an obvious effect on both the polymerization and the resulting polymer. Increasing [PDO]/[*t*-BuP_4] ratios facilitated the molecular weight growth, whereas the conversions of PDO significantly decreased. © 2015 Wiley Periodicals, Inc. J. Appl. Polym. Sci. **2016**, *133*, 43030.

KEYWORDS: biodegradable; catalysts; polyesters

Received 7 April 2015; accepted 9 October 2015
DOI: 10.1002/app.43030

INTRODUCTION

Polyesters are receiving increasing attention owing to their outstanding biodegradable,[1–3] biocompatible,[1,4] and environment-friendly properties.[5] These materials have wide applications in environmental and biomedical engineering.[6–9] By now, numerous polyesters such as polyglycolide (PGA),[6] polylactide (PLA),[2,10] and poly(ε-caprolactone) (PCL)[11,12] have been prepared. Among them, poly(*p*-dioxanone) (PPDO) has attracted significant interest owing to its excellent physical properties and outstanding biodegradability.[5,13–18] PPDO shows a greater flexibility and hydrophilicity with respect to PGA and PLA because of the coexistence of ester and ether bonds in the molecular structure.[17,18] Furthermore, PPDO has proven to be tougher than PLA and even high-density polyethylene with a tensile strength of approximately 7000 psi for an ultimate elongation ranging from 500% to 600%.[19] More importantly, PPDO can completely degrade in body within a period of 180 days, making it to be a potential candidate for medical use.[20]

In general, PPDO can be synthesized by the ring-opening polymerization (ROP) of *p*-dioxanone (PDO) using metallic catalysts such as tin(II) bis(2-ethylhexanic acid), triethylaluminum, aluminum alkoxides, zinc derivatives, ferric alkoxides, titanium alkoxides, and yttrium complexes.[21–26] Because PPDO has potential applications in the biomedical and pharmaceutical industries either as biodegradable implants or in controlled drug-delivery systems, it is necessary to remove all the traces of the metallic residues. However, the metallic catalyst is hard to remove, and the procedure is tedious. The metal-free catalyst used for its preparation seems to be an effective means to solve this problem. However, by now, only a few nonmetallic catalysts such as immobilized lipase CA and some organolanthanide complexes were explored,[27,28] and search for more effective catalysts for metal-free PPDO is still a big challenge.

This study aims at to find a metal-free catalyst for the ROP of PDO. Herein, 1-*tert*-butyl-4,4,4-tris(dimethylamino)-2,2-bis[tris-(dimethylamino)-phosphoranylidenamino]-2Λ^5,4Λ^5-catenadi(phosphazene) (*t*-BuP_4) was used as the catalyst for the ROP of ethylene oxide and *β*-lactam or the anionic polymerization of vinyl monomers.[29–34] Moreover, the effects of polymerization conditions and the mechanism were studied in detail. We believe

that this method may offer innovative insights into the synthesis and applications of PPDO.

EXPERIMENTAL

Materials

PDO was provided by Jlight Chemicals Company (China) and dried for 48 h over calcium hydride (CaH_2) at room temperature under reduced pressure (100 Pa). Then, it was distilled under reduced pressure before use (40 Pa, 70°C). 1,4-Butanediol (BDO) purchased from Sinopharm was distilled in the presence of Na_2SO_4 under reduced pressure. Benzyl alcohol (BA) from Aldrich was dried over sodium under a nitrogen protective atmosphere and distilled under vacuum after refluxing for hours. Aniline was dried over KOH or CaH_2 and distilled under reduced pressure. *t*-BuP_4 was purchased from Sigma-Aldrich and used as received. Other reagents from Sinopharm were used as received.

Characterizations

^{1}H NMR spectra were recorded using a Bruker AV400 NMR spectrometer using $CDCl_3$ as the solvent and tetramethylsilane (TMS) as the internal standard.

Intrinsic viscosity was measured using a Ubbelohde viscometer in phenol/1,1,2,2-tetrachloroethane (1/1 v/v) mixture at 30°C. Viscosity-average molecular weights (M_vs) of PPDO were calculated using the Mark–Houwink equation $[\eta] = KM^{\alpha}$ ($\alpha = 0.63$, $K = 7.9 \times 10^4$ mL/g).[35]

The number and weight-average molecular weights (M_n and M_w) and polydispersity (PDI) were determined by gel permeation chromatography (GPC) at 35°C using a Waters 1515 HPLC pump using a series of monodisperse polystyrenes as the standard and chloroform ($CHCl_3$) containing 0.3 wt % tri-*n*-octylmethylammonium chloride as the fluent at a flow rate of 1.0 mL/min.

Thermogravimetric analysis (TGA) was performed using a TA SDT Q600 thermogravimetric analyzer under nitrogen atmosphere at a heating rate of 10°C/min in the range 25°C–500°C.

Differential scanning calorimetry (DSC) was performed using a DSC Q2000 analyzer at a nitrogen flow rate of 50 mL/min. Samples were quickly heated to 150°C and kept for 10 min to remove thermal history, then cooled to −50°C at a rate of 10°C/min. Finally, they were reheated to 150°C at the same rate.

Matrix Assisted Laser Desorption/Ionization Time of Flight Mass Spectroscopy (MALDI-TOF MS) was performed on a Biflex III spectrometer (Bruker-Franzen Analytik).

ROP of PDO Catalyzed by *t*-BuP_4

The polymerization was performed in a 5 mL vial with a magnetic stirrer. The vial was flame dried and subjected to an alternating vacuum-nitrogen purge cycle of three cycles. Then, PDO, initiator (alcohol or aniline), and *t*-BuP_4 were introduced under nitrogen atmosphere. Thereafter, the vial was sealed, and the polymerization was performed at the set polymerization temperature for a certain time. Then, the solution was poured in a large amount of phenol/1,1,2,2-tetrachloroethane (1/1 v/v) mixture. The resulting polymer was collected, washed with the acetone/water mixture, and dried in vacuum.

RESULTS AND DISCUSSION

Phosphazene base *t*-BuP_4 is usually used as a catalyst for the ROP of ethylene oxide and/or lactam. In particular, it can catalyze a hybrid copolymerization of ε-caprolactone and methyl methacrylate.[31,32] All these polymerizations refer to anionic living species, following the anionic polymerization mechanism. Based on these studies, *t*-BuP_4 was expected to deprotonate the nucleophilic initiators (such as alcohol) form anionic living species to initiate the ROP of PDO, yielding metal-free biocompatible PPDO. For this purpose, *t*-BuP_4 was first used to catalyze the ROP of PDO at 80°C at a fixed [BDO]/[*t*-BuP_4] molar ratio of 1:1, and BDO was used as the initiator.

Figure 1 shows the ^{1}H NMR spectrum of PPDO. After the polymerization, the signals assigned to —OCH_2CH_2OCO—, —COCH_2O—, and —OCH_2CH_2OCO— of PDO in the ranges at 3.82–3.90, 4.31–4.39, and 4.45–4.51 ppm were shifted in the ranges at 3.77–3.82, 4.14–4.21, and 4.30–4.37 ppm, respectively, indicating that *t*-BuP_4 successfully catalyzed the ROP of PDO, forming metal-free PPDO. The signals of the —OCH_2CH_2CH_2CH_2O— of BDO appeared at 1.49 − 1.51 ppm. However, the signals due to the −OCH_2CH_2CH_2CH_2O– of BDO were overlapped by PDO units. Moreover, the different chemical shifts for the protons of PDO and PPDO were helpful in estimating the conversions of PDO ($Conv._{PDO}$) according to the integrals calculated from the ^{1}H NMR spectra.

After confirming that *t*-BuP_4 catalyzed the ROP of PDO, the effect of reaction temperature on the polymerization was studied by fixing the reaction time for 48 h and at the molar ratio of [PDO]/[BDO]/[*t*-BuP_4] at 200:1:1. Not all the polymers can dissolve in $CHCl_3$, therefore, M_vs were used to characterize the polymer, and the corresponding GPC and polydispersity data are listed in Table I.

As shown in Figure 2, when the polymerization was conducted at 40°C, only 5.6% of PDO was consumed. Increasing temperature from 40°C to 100°C, $Conv._{PDO}$ increased and finally reached a maximum of 88.7%, which is close to the value reported by Wang *et al.* using metallic catalysts and significantly higher than that using enzymes as catalyst.[8] The M_v of the corresponding polymer was 2.09×10^4 g/mol, which is lower than the molecular weights reported for metal-catalyzed PPDO. Further increase in the temperature to 120°C decreased both the $Conv._{PDO}$ (54.4%) and M_v (1.46×10^4 g/mol), indicating that the optimal temperature of approximately 100°C was necessary for the ROP of PDO. Three probable reasons are elucidated as follow. First, PPDO is a semicrystalline polymer with a melting temperature (T_m) of approximately 110°C. Increasing polymerization temperature avoided the deactivation of the active species caused by the crystallization during the polymerization. This could be evidenced by the gradual opacity of the reaction medium. Moreover, high temperature also favors the monomer diffusion and initiation. However, the ROP of PDO was in thermodynamic equilibrium between the polymerization and the depolymerization. Conducting the polymerization at high temperature shifted the thermodynamic equilibrium toward the depolymerization, resulting in a low monomer conversion and polymer with a low molecular weight.

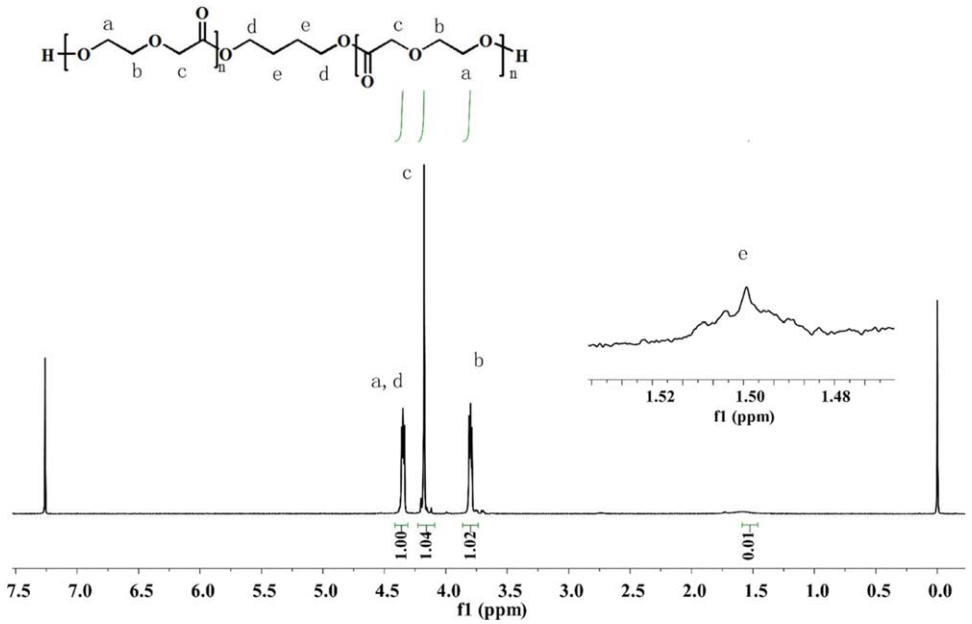

Figure 1. ^{1}H NMR spectrum of PPDO synthesized in bulk at 80°C using BDO as the initiator and the [PDO]/[BDO]/[*t*-BuP$_4$] ratio of 200:1:1. [Color figure can be viewed in the online issue, which is available at wileyonlinelibrary.com.]

Figure 3 shows the effect of the reaction time on *Conv.*$_{PDO}$s and M_vs at 80°C at 200:1:1 molar ratio of [PDO]/[BDO]/[*t*-BuP$_4$]. This bulk polymerization proceeded homogeneously until 20 h. After that, the polymeric system became opaque, indicating the occurrence of crystallization. Clearly, both the *Conv.*$_{PDO}$ and M_v of PPDO increased with time within 48 h, whereas when the polymerization time was extended from 48 to 72 h, the rate of increase in the *Conv.*$_{PDO}$ and M_v of PPDO became slow. Finally, M_v of PPDO reached 2.04 × 10^4 g/mol, and 70.4% of *Conv.*$_{PDO}$ was obtained.

Figure 4 shows the GPC traces of the polymers at different reaction times. Because the polymer obtained at 72 h did not dissolve completely in $CHCl_3$, no signal for this polymer was

Table I. ROP of PDO Using Different Initiators

Sample	XH	PDO:XH:*t*-BuP$_4$	T^a (°C)	t^b (h)	*Conv.*$_{PDO}$ (%)	$M_v \times 10^{-4}$ (g/mol)	$M_n \times 10^{-4}$ (g/mol)	PDI	χ^c (%)
PPDO-1	BDO	200:1:1	40	72	5.6	0.14	0.21	2.86	
PPDO-2	BDO	200:1:1	60	72	17.2	0.96	0.67	2.64	
PPDO-3	BDO	200:1:1	80	72	70.4	2.04	-	-	0.41
PPDO-4	BDO	200:1:1	100	72	88.7	2.09	-	-	
PPDO-5	BDO	200:1:1	120	72	54.4	1.46	1.73	3.13	
PPDO-6	BDO	200:1:1	80	1	5.5	0.65	0.48	2.27	
PPDO-7	BDO	200:1:1	80	3	8.7	0.76	0.71	2.30	
PPDO-8	BDO	200:1:1	80	6	11.6	0.93	0.66	2.98	
PPDO-9	BDO	200:1:1	80	18	24.6	1.09	0.91	2.90	
PPDO-10	BDO	200:1:1	80	48	60.2	1.94	1.61	2.65	
PPDO-11	BDO	80:1:1	80	72	84.2	1.34	1.59	2.38	
PPDO-12	BDO	100:1:1	80	72	79.8	1.40	1.70	2.61	
PPDO-13	BDO	500:1:1	80	72	62.4	2.78	-	-	
PPDO-14	BDO	1000:1:1	80	72	44.7	2.81	-	-	
PPDO-15	Aniline	200:1:1	80	72	69.8	1.87	2.11	3.05	0.39
PPDO-16	-	200:-:1	80	72	24.6	0.67	0.55	2.91	0.20
PPDO-17	BA	200:1:1	80	72	82.3	2.77	-	-	

[a] Reaction temperature.
[b] Reaction time.
[c] The parentheses the degrees of crystallinity determined using the melting of 14.4 kJ/mol for 100% crystalline PPDO.

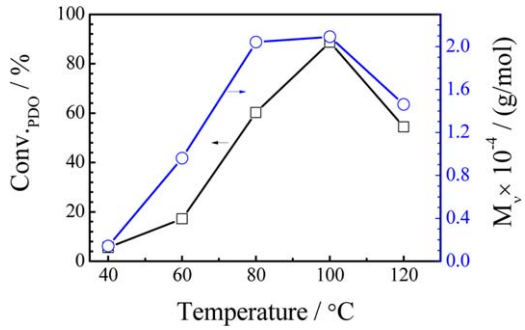

Figure 2. Temperature dependence of $Conv._{PDO}$s and M_vs under a fixed reaction time 48 h and the [PDO]/[BDO]/[*t*-BuP$_4$] ratio of 200:1:1. [Color figure can be viewed in the online issue, which is available at wileyonlinelibrary.com.]

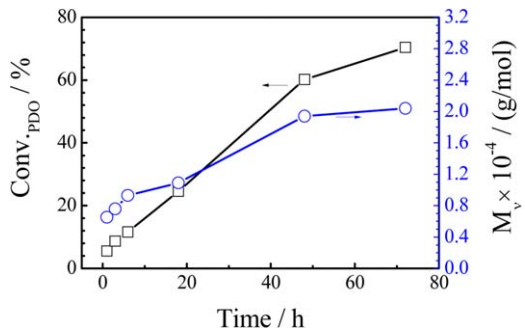

Figure 3. Time dependence of $Conv._{PDO}$s and M_vs, ([PDO]/[BDO]/[*t*-BuP$_4$] = 200:1:1, 80°C). [Color figure can be viewed in the online issue, which is available at wileyonlinelibrary.com.]

observed. As shown in Figure 4, the GPC traces shifted toward high molecular weight with increasing reaction time, indicating the living characteristic of the polymerization. Detailed studied on the GPC traces indicated that the polymer distributions were monomodal at the reaction time in the range 1 to 6 h. However, with further increase in the reaction time, the GPC traces became much wider and asymmetrical. At 48 h, an obvious shoulder was observed in the high-molecular-weight region. This may be attributed the occurrence of a transesterification reaction.

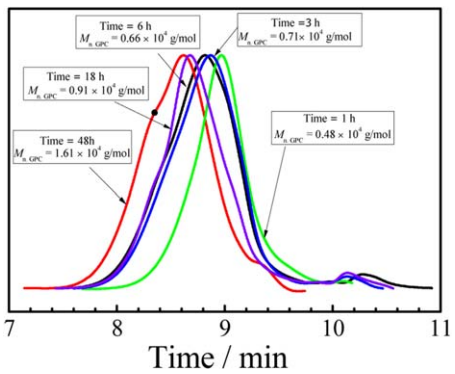

Figure 4. GPC traces from differential refractive index (DRI) detector of the polymers at different reaction times, ([PDO]/[BDO]/[*t*-BuP$_4$] = 200:1:1). [Color figure can be viewed in the online issue, which is available at wileyonlinelibrary.com.]

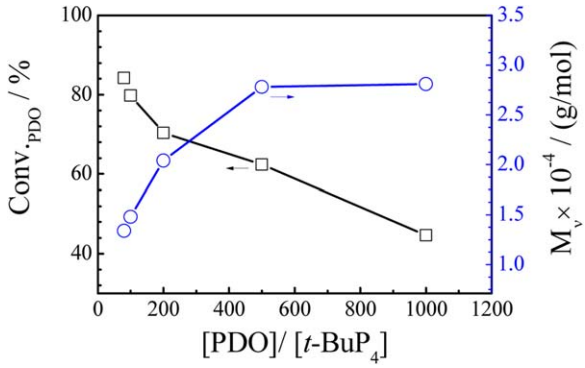

Figure 5. Feed ratio dependence of $Conv._{PDO}$s and M_vs under a fixed reaction time of 48 h at 80°C. [Color figure can be viewed in the online issue, which is available at wileyonlinelibrary.com.]

Figure 5 shows the effect of the catalyst on the polymerization at varying [PDO]/[*t*-BuP$_4$] molar ratios from 80 to 1000. The reaction time was fixed for 48 h at a reaction temperature of 80°C. The molar ratio of [BDO]/[t-BuP$_4$] was fixed at 1:1. The molar ratios of [PDO]/[*t*-BuP$_4$] had an obvious effect both on the $Conv._{PDO}$ and M_v. With increasing [PDO]/[*t*-BuP$_4$] ratio from 80 to 500, $Conv._{PDO}$ decreased from 84.2% to 44.7%. In contrast, M_v increased from 1.34 × 10^4 to 2.79 × 10^4 g/mol. However, with further increase in the [PDO]/[*t*-BuP$_4$] ratio from 500 to 1000, no apparent increasing in M_v was observed. This is because the concentration of initiator was constant with respect to the catalyst. Using high [PDO]/[*t*-BuP$_4$] ratio indicated much more numbers of monomer incorporating into the same polymer chains, resulting in PPDO with high M_v. When the [PDO]/[*t*-BuP$_4$] ratio was too high, the concentration of active centers was too limited, thus obviously decreased the monomer conversions, indicating that the optimum [PDO]/[*t*-BuP$_4$] ratio for the ROP of PDO was approximately 500.

In this study, BDO was used as the initiator. However, the end groups of the resulted PPDOs were hard to characterize by NMR because of the overlap of the corresponding signals for the initiator and PDO segments in the polymers. Hence, BA was employed as an initiator. Figure 6 shows the ^{1}H NMR spectrum of PPDO initiated by BA. Obviously, the signals assigned to phenyl and —CH_2O protons of the BA were observed in the range 7.28–7.30 and 5.19–5.21 ppm, indicating the existence of the BA moieties at the end of the polymer chain.

Scheme 1 shows a proposed mechanism of the ROP of PDO catalyzed by *t*-BuP$_4$ in the presence of BA as the initiator as an example. First, BA is deprotonated by *t*-BuP$_4$ forming the corresponding anion, which continuously reacts with the monomers to yield oxygenated anions. Finally, the oxygenated anions further attack the carbonyl carbon of PDO to afford the polymers. The polymerization follows characteristic anionic living polymerization. Notably, the transesterification reaction might take place during the polymerization, especially at high conversion of the monomer. The termination might occur through the deactivating the living center. Both of them would result in broad polydispersitis.

This ROP mechanism of PDO was further supported by the MALDI-TOF MS spectrum of the PPDO oligomer synthesized

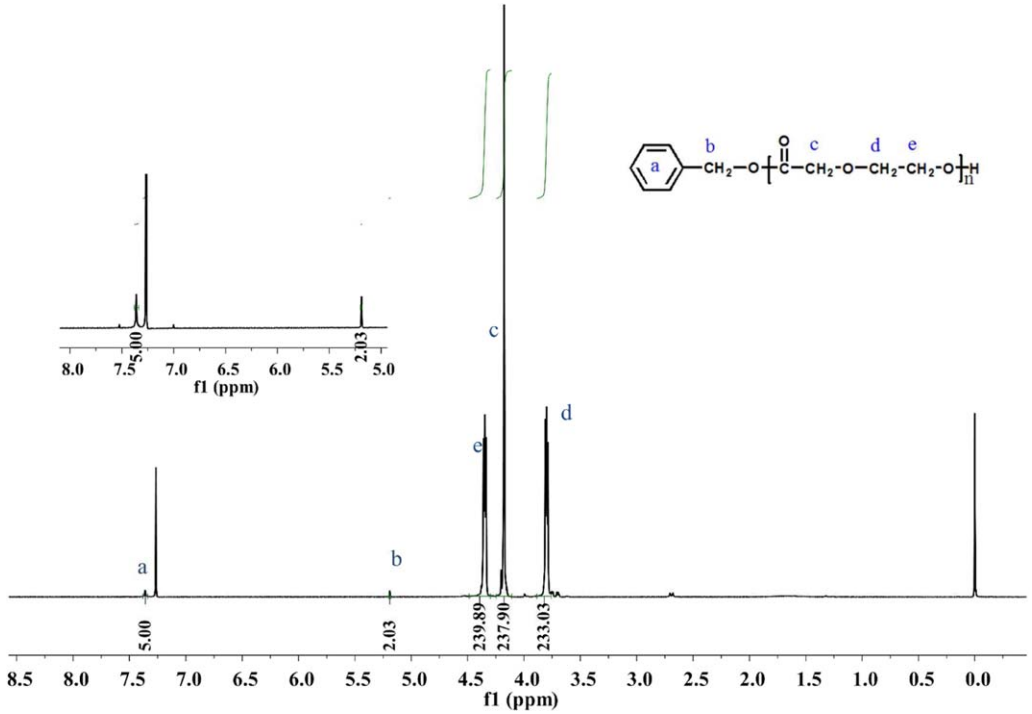

Figure 6. ^{1}H NMR spectrum of PPDO synthesized in bulk at 80°C using benzyl alcohol (B) as the initiator. ([PDO]/Benzyl alcohol]/[*t*-BuP$_4$] = 200:1:1). [Color figure can be viewed in the online issue, which is available at wileyonlinelibrary.com.]

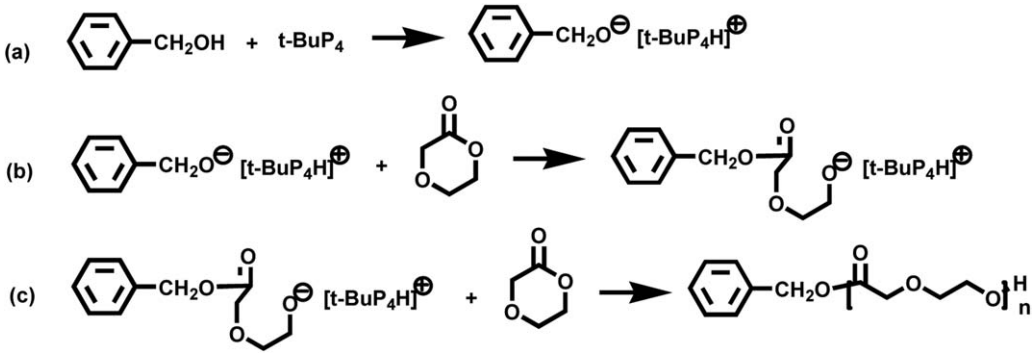

Scheme 1. Proposed mechanism for the ROP of PDO catalyzed by *t*-BuP$_4$ in the presence of BA as the initiator.

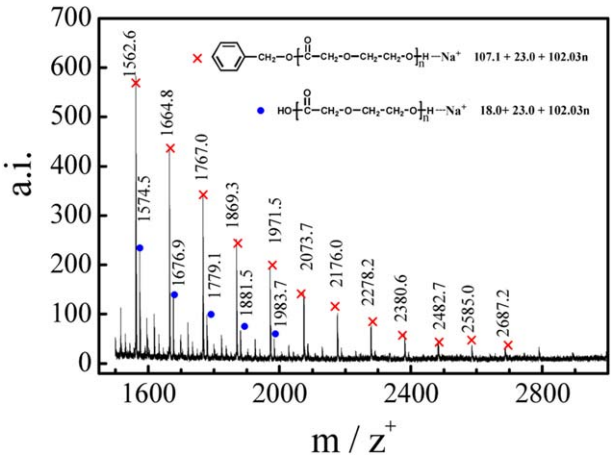

Figure 7. MALDI-TOF mass spectrum of PPDO initiated by benzyl anchol ([PDO]/[BA]/[t-BuP4] = 30:1:1). [Color figure can be viewed in the online issue, which is available at wileyonlinelibrary.com.]

in a [PDO]/[BA] ratio of 30. As shown in Figure 7, two series of signals could be identified. One was due to the telechelic structure with BA in the polymer backbone. The other could be caused by traces of water during the polymerization, which was confirmed by the experiment without addition of any alcohol. In this case, trace amount of water in the system was activated by *t*-BuP$_4$, used as the initiator. However, both the $Conv._{PDO}$ and M_v were very low (Table I).

Aniline was also used to initiate the ROP of PDO, in which 69.8% of PDO was consumed, and a polymer with M_v of 1.87 × 10^4 g/mol was obtained. Figure 8 shows the ^{1}H-NMR spectrum of PPDO initiated by aniline. The signals attributed to the phenyl protons of the initiator are observed in the range of approximately 7.25–7.33 ppm, indicating the existence of the aniline moieties at the end of the polymer chain. The conclusion is important because it indicates that the end groups of polymer can be easily tailored by using different types of initiators, which is hard to achieve by conventional synthesis for PPDO.

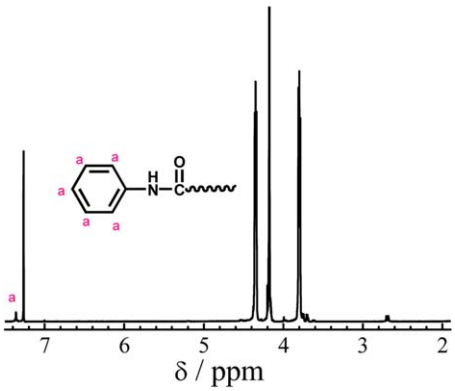

Figure 8. ^{1}H NMR spectrum of PPDO synthesized in bulk at 80°C using aniline as the initiator ([PDO]/[Aniline]/[t-BuP$_4$] = 200:1:1). [Color figure can be viewed in the online issue, which is available at wileyonlinelibrary.com.]

Figure 9 shows the cooling and second heating curves for the PPDO synthesized using different initiators, and the data are listed in Table I (PPDO-3, PPDO-15, and PPDO-16). The cooling scans [Figure 9(a)] exhibit the crystallization exothermal peak at approximately 33°C −61°C. The degree of crystallinity (χ%) was obtained from the experimentally determined value for the heat of fusion (ΔH_m) divided by the heat of fusion of 100% crystalline PPDO (ΔH_m^0), which is 14.4 kJ/mol as determined by Wunderlich and coworkers.[35] Herein, the degree of crystallinity for PPDO-3 and PPDO-15 were 0.41 and 0.39, respectively, which are much greater than that for PPDO-16 (0.20). This is may be attributed the low molecular weight of PPDO-16 (Table I). A weak glass transition temperature (T_g) was observed for the second heating scan [Figure 9(b)]. The T_g

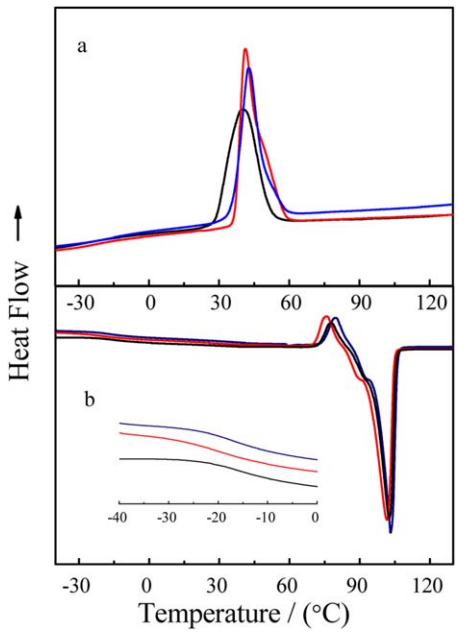

Figure 9. DSC curves for PPDO-3 (*red*), PPDO-15(*blue*), and PPDO-16(*black*) in the cooling (**up**) and the second heating run (**down**) at a heating rate of 10°C/min. [Color figure can be viewed in the online issue, which is available at wileyonlinelibrary.com.]

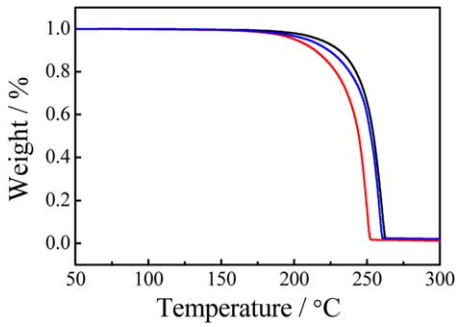

Figure 10. TGA curves for PPDO-3 (*black*), PPDO-15 (*blue*), and PPDO-16 (*red*) at a heating rate of 10°C/min. [Color figure can be viewed in the online issue, which is available at wileyonlinelibrary.com.]

values for PPDO-3, PPDO-15, and PPDO-16 were −19.03, −19.22, and −21.28°C, respectively. The weak T_g values were because of the high crystallinity of the PPDO polymers.

Figure 10 shows the TGA curves of PPDO-3, PPDO-15, and PPDO-16 at a heating rate of 10°C/min. It can be seen that PPDO-3 and PPDO-15 have a similar thermal stability, in which weight change on thermo balances were detectable approximately 189°C and decreased smoothly up to nearly complete degradation approximately 267°C. For PPDO-16, the starting temperature for the thermal degradation was approximately 180°C, which was close to those of PPDO-3 and PPDO-15. However, the complete decomposition temperature was only 250°C, which was significantly lower than those of PPDO-3 and PPDO-15. The reason might be because of the low molecular weight of PPDO-16.

CONCLUSIONS

In summary, a series PPDOs were successfully synthesized by the ROP of PDO using a metal-free catalyst. The monomer conversions and M_vs of the polymer increased with the increase in temperature within 100°C. Further increase in the temperature decreased the M_vs of the polymers. Both the monomer conversions and the M_vs of the polymers increased with polymerization time and finally reached to maximum values. The optimum [PDO]/[*t*-BuP$_4$] ratio for the polymerization was approximately 500. Addition of alcohol or aniline used as the initiator was necessary for the polymerization. Without any initiator, trace amount of water in the system might be activated by *t*-BuP$_4$; however, both the conversion of PDO and the M_vs of resultant PPDOs were limited.

ACKNOWLEDGMENTS

The financial supports of this work by the National Natural Science Foundation of China (Nos. 21174020 and 21304010), the Natural Science Foundation of Jiangsu Province (BK20130246), the Priority Academic Program Development of Jiangsu Higher Education Institutions (PAPD) and the Program of Innovative Research Team of Changzhou University (ZMF13020026).

REFERENCES

1. Wu, L. B.; Ding, J. D. *Biomaterials* **2004**, *25*, 5821.
2. Kricheldorf, H. R.; Kreiser-saunders, I.; Boettcher, C. *Polymer* **1995**, *36*, 1253.
3. Yu, X.; Feng, J.; Zhuo, R. *Macromolecules* **2005**, *38*, 6244.
4. Raquez, J. M.; Degee, P.; Narayan, R.; Dubois, P. *Macromol. Rapid Commun.* **2000**, *21*, 1063.
5. Vilela, C.; Sousa, A. F.; Fonseca, A. C.; Serra, A. C.; Coelho, J. F.; Freire, C. S.; Silvestre, A. J. *Polym. Chem.* **2014**, *5*, 3119.
6. Tempelaar, S.; Mespouille, L.; Coulembier, O.; Dubois, P.; Dove, A. P. *Chem. Soc. Rev.* **2013**, *42*, 1312.
7. Albertsson, A.; Varma, I. K. *Biomacromolecules* **2003**, *4*, 1466.
8. Liu, G. Y.; Zhai, Y. L.; Wang, X. L.; Wang, W. T.; Pan, Y. B.; Dong, X. T.; Wang, Y. Z. *Carbohydr. Polym.* **2008**, *74*, 862.
9. Remant Bahadur, K.; Aryal, S.; Raj Bhattarai, S.; Seob Khil, M.; Kim, H. *J. Appl. Polym. Sci.* **2007**, *103*, 2695.
10. Cohn, D.; Salomon, A. *Biomaterials* **2005**, *26*, 2297.
11. Karjalainen, T.; Hiljanen-Vainio, M.; Malin, M.; Seppala, J. B. *J. Appl. Polym. Sci.* **1996**, *59*, 299.
12. Asandei, A. D.; Chen, Y. H.; Adebolu, O. I.; Simpson, C. P. *J. Polym. Sci., Part A: Polym. Chem.* **2008**, *46*, 2869.
13. Albertsson, A. C.; Varma, I. K. *Adv. Polym. Sci.* **2002**, *157*, 1.
14. Yan, Y.; Siegwart, D. J. *Polym. Chem.* **2014**, *5*, 1362.
15. Pack, J. W.; Kim, S. H.; Choi, I.-W.; Park, S. Y.; Kim, Y. H. *J. Polym. Sci., Part A: Polym. Chem.* **2007**, *40*, 544.
16. Chen, S. C.; Zhou, Z. X.; Wang, Y. Z.; Wang, X. L.; Yang, K. K. *Polymer* **2006**, *47*, 32.
17. Li, F.; Feng, J.; Zhuo, R. *J. Appl. Polym. Sci.* **2006**, *102*, 5507.
18. Redin, T.; Finne-Wistrand, A.; Mathisen, T.; Albertsson, A. C. *J. Polym. Sci., Part A: Polym. Chem.* **2007**, *45*, 5552.
19. Doddi, N.; Versfelt, C. C.; Wasserman, D. U.S. Pat. 4,052,988[P], **1977**.
20. Lin, H. L.; Chu, C. C.; Grubb, D. *J. Biomed. Mater. Res.* **1993**, *27*, 153.
21. Zhu, J.; Dong, X. T.; Wang, X. L.; Wang, Y. Z. *Carbohydr. Polym.* **2010**, *80*, 350.
22. Sugih, A. K.; Picchioni, F.; Heeres, H. J. *Eur. Polym. J.* **2009**, *45*, 155.
23. Raquez, J. M.; Degee, P.; Narayan, R.; Dubois, P. *Macromolecules* **2001**, *34*, 8419.
24. Zeng, J. B.; Srinivansan, M.; Li, Y. D.; Narayan, R.; Wang, Y. Z. *J. Polym. Sci., Part A: Polym. Chem.* **2010**, *48*, 5885.
25. Zhu, X. L.; Wu, G.; Qiu, Z. C.; Zhou, Y.; Gong, J.; Yang, K. K.; Wang, Y. Z. *J. Polym. Sci., Part A: Polym. Chem.* **2008**, *46*, 5214.
26. Ding, S. D.; Bai, C. Y.; Liu, Z. P.; Wang, Y. Z. *J. Therm. Anal. Calorim.* **2008**, *94*, 89.
27. Zeng, T.; Wang, Y.; Shen, Q.; Yao, Y.; Luo, Y.; Cui, D. *Organometallics* **2014**, *33*, 6803.
28. Chen, R.; Zhang, Y.; Wang, Y. *J. Mol. Catal. B: Enzym.* **2009**, *57*, 224.
29. Schwesinger, R.; Hasenfratz, C.; Schlemper, H.; Walz, L.; Peters, E. M.; Peters, K.; Schnering, H. G. *Angew. Chem. Int. Ed. Engl.* **1993**, *32*, 1361.
30. Zhao, J. P.; Hadjichristidis, N.; Gnano, Y. *Polymer* **2014**, *59*, 49.
31. Yang, H. J.; Xu, J. B.; Pispas, S.; Zhang, G. Z. *Macromolecules* **2012**, *45*, 3312.
32. Yang, H. J.; Xu, J. B.; Zhang, G. Z. *Sci. China Chem.* **2013**, *56*, 1.
33. Misaka, H.; Sakai, R.; Satoh, T.; Kakuchi, T. *Macromolecules* **2011**, *44*, 9099.
34. Chen, Y.; Fuchise, K.; Narumi, A.; Kawaguchi, S.; Satoh, T.; Kakuchi, T. *Macromolecules* **2011**, *44*, 9091.
35. Sabino, M. A.; Feijoo, J. L.; Muller, A. *J. Macromol. Chem. Phys.* **2000**, *201*, 2687.